JOURNAL OF AIRCRAFT
Vol. 41, No. 2, March–April 2004

Study of Multirow Highly Loaded Bolt Joints in Composite Wing Structure

Hsien-Yang Yeh,* Johnathan J. Lee,† and Daniel Y. T. Yang‡
California State University, Long Beach, Long Beach, California 90840
and
Hsien-Liang Yeh§
I-Shou University, Kaohsiung County 84008, Taiwan, Republic of China

The purpose of this study is to develop reliable methods for the design, analysis, and evaluation of multirow highly loaded bolt joints of composite structures. Several different fastener flexibility evaluation methods are compared for the single-shear and double-shear joints with fasteners of various types and sizes. The design specimens used in this study were made from stitched/resin film-infused carbon fiber composite material, and the load intensities were on the order of 50 to 60 kips per in. (87598.5 to 105118.2 N/cm), within the specimen width for 0.94-in. (2.39 cm) thick pad-up skin. Linear and nonlinear finite element analyses were performed on both compression and tension high-load specimens. Actual tests were performed, and results are compared with the predictions from the finite element analysis model. As the results indicate, in composite structures the uniform bolt loading is crucial to the design and flexibility calculations of multirow highly load bolt joints.

Nomenclature

A_b	=	bolt area
a	=	semi-empirical values depend on fastener material
b	=	semi-empirical values depend on fastener material
C_{bb}	=	flexibility caused by bolt bending deformation
C_{bbr}	=	flexibility caused by bolt bearing deformation
C_{bs}	=	flexibility caused by shear deformation
C_{pbr}	=	flexibility caused by plates bearing deformation
D	=	diameter of the fasteners
E_{bbr}	=	Young's modulus of the bolt
E_L	=	modulus of elasticity of side member (1 or 2) in longitudinal direction
E_s	=	Youngs modulus of fastened material
E_T	=	modulus of elasticity of side member (1 or 2) in transverse direction
F	=	joint flexibility
F_{RB}	=	bolt flexibility
F_{RS}	=	fastened material flexibility
G_b	=	shear modulus of elasticity of the bolt
K	=	joint stiffness
P	=	applied load
t_1, t_2	=	thickness of fastened material
β	=	fixity coefficient, varies from 0 (complete fixity) to 1 (no fixity)
δ	=	joint displacement

Introduction

AIRCRAFT structural components are usually very large. Many airplane parts must be arranged so that they can be disassembled for shipping, inspection, repair, and replacement. Fasteners are always used to join different parts together. In general, joints are perhaps the most common source of failure in aircraft structures, and therefore it is important that all aspects of joint design are given consideration in the structural analysis.

This study describes the method of analysis for highly loaded bolted joints in composite wing structures. Two different designs were used in single-shear (high-load compression specimen) and double-shear (high-load tension specimen) joints. Finite element analysis was used to verify and validate the effectiveness of the semi-empirical methodology. The importance of fastener flexibility on bolts is also discussed here, and several flexibility equations and fastener types for double- and single-shear bolted joints are compared.

Finally, tests were performed on the high-load compression specimen, and the results were compared with the predictions from the finite element analysis model. The results indicate that in composite structures the uniform bolt loading is crucial to the design and flexibility calculations of multirow highly loaded bolt joints.

Specimen Design

High-Load Tension Specimen

The double-shear tension joint test specimen [sized to handle 60 kips/in. (105118.2 N/cm)] is shown in Fig. 1. This test specimen was chosen to evaluate the maximum load-carrying capability of a stitched/resin film-infused (S/RFI) panel at the most critical region of the wing. The tension joint has four rows of bolts (perpendicular to the line of loading) in three columns (parallel to the line of loading) between each stringer [8-in. (20.32 cm) spacing] with a total of 11 fasteners. Two different bolt diameters are used: $\frac{5}{8}$ in. (1.59 cm), and $\frac{3}{4}$ in. (1.9 cm).

The high load double-shear tension specimen is composed of an aluminum outer-moldline (OML) splice plate and inner-moldline (IML) splice tee, sandwiching the built-up composite wing skins of the center and outer wing cover panel. These two splice plates provide a fail-safe load path should one plate develop a tension crack. The splice plates are also designed to have small eccentricities at the panel joint, thereby minimizing the secondary bending effect.

High-Load Compression Specimen

The single-shear compression joint test specimen [sized to handle 50 kips/in. (87598.5 N/cm)] is shown in Fig. 2. The specimen has five rows of bolts (perpendicular to the line of loading) in three columns (parallel to the line of loading) between each stringer [8-in. (20.32 cm) spacing] with 14 fasteners. Three different bolt diameters are used: $\frac{1}{2}$, $\frac{5}{8}$, and $\frac{3}{4}$ in. (1.27, 1.59, and 1.9 cm).

Received 22 June 2001; revision received 18 January 2003; accepted for publication 7 February 2003.

*Professor, Department of Mechanical and Aerospace Engineering.
†Graduate Student, Department of Mechanical and Aerospace Engineering.
‡Graduate Student, Department of Mechanical and Aerospace Engineering.
§Professor, Department of Civil Engineering.

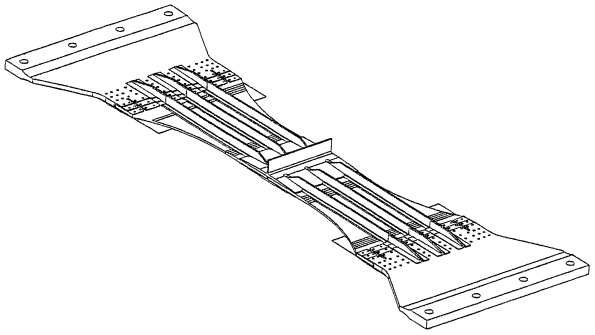

Fig. 1 High-load tension panel test specimen.

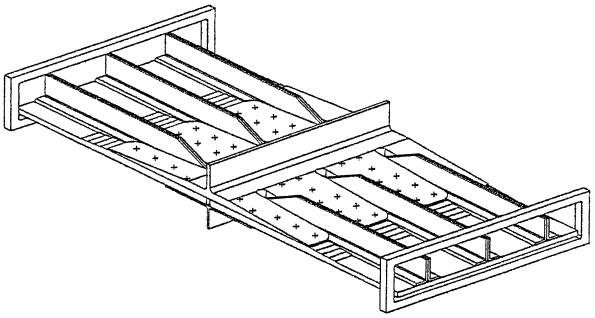

Fig. 2 High-load compression panel test specimen.

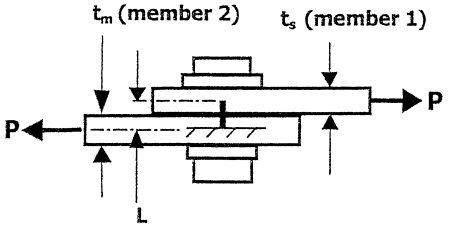

Fig. 3 Finite elment bolt model of single-shear joint.

The single-shear compression specimen is composed of a primary aluminum IML splice plate and secondary OML flex tee, which sandwiches the built-up composite wing skins of the center and outer wing cover panel. The panel and splice plates were also designed to have small eccentricities at the panel joint, thereby minimizing the secondary bending effect.

Fastener Flexibility

Joint flexibility is a prominent parameter in the design and analysis of multirow highly loaded composite bolted joints because it is important to know the bolt load distribution of these joints. A reasonable estimation of fastener flexibility in the bolted composite joints is vital to understand the load transfer, load distribution, and durability at the joints. Again, different analyses were done on both the single-shear joint and the double-shear joint.

Single-Shear Joint

Many joint flexibility empirical equations were established, based on the testing data of the single-shear metallic splice joint.[1,2] In finite element modeling (FEM) of single-shear joints, bolts are modeled as single bar elements, connecting the side of the plate (member 1) to the main plates (member 2), as shown in Fig. 3.

Swift equation[1]:

$$F = \frac{1}{K} = \frac{a}{\left(\dfrac{\sqrt{E_{1L} + E_{1T}} + \sqrt{E_{2L} + E_{2T}}}{2}\right)D} + b\left(\frac{1}{\sqrt{E_{1L} + E_{1T} t_1}} + \frac{1}{\sqrt{E_{2L} + E_{2T} t_2}}\right)$$

Table 1 Stiffness comparison for single-shear head flush fastener joint

Specimen (composite titanium bolt): $t_1 = 0.462$ in. (1.17 cm) $t_2 = 0.25$ in. (0.64 cm) $D = \frac{3}{8}$ in. (0.95 cm) diam	Swift equation	Hadcock equation	Hart–Smith modified NACA equation	Test data[2]
Spring rate K, lb/in.	−847,200	413,600	499,100	690,000
(N/cm)	−1484294.4	724627.2	874423.2	1208880
Deviation rate	+27%	−60%	−38%	——

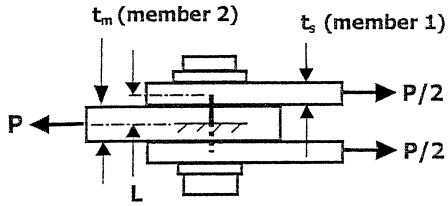

Fig. 4 Finite element bolt model of double-shear joint.

$$F = F_{RB} + F_{RS}$$

Hadcock equation[2]

$$F = \frac{1}{K} = \frac{\delta}{P} = \frac{(t_1 + t_2)^2}{E_B D^3} + 3.72\left(\frac{1}{t_1\sqrt{E_{1L}E_{1T}}} + \frac{1}{t_2\sqrt{E_{2L}E_{2T}}}\right)$$

Reference 2 indicates that the Swift equation overestimates the overall stabilizer joint by 23% and the Hadcock equation underestimates the overall stiffness of the joint by 60%. Testing results, of a typical composite-titanium plate with titanium bolted joints, show that the spring rate (overall joint stiffness) is approximately 690,000 lb/in. (1208880 N/cm) for $\frac{3}{8}$-in. (0.95 cm)-diam bolts connecting the $\frac{1}{4}$-in. (0.64 cm) thick titanium plate and the 0.642-in. (1.63 cm) thick hybrid composite laminate.[1]

The most well-known and widely used flexibility equation in the industry today is derived by using a semi-empirical approach.[3,4] However, this equation is based on symmetrical butt (double-shear) joints of metallic structures, and minor modification is necessary for single-shear joints, especially for fibrous composite materials. Hart–Smith modified this equation to account for the bolt rotation that occurs in single-shear joints.[5] The second term of this equation, accounting for bolt bending, was deleted, and the remaining three terms were all multiplied by the factor $(1 + 3\beta)$ representing the fraction of eccentric moment on the bolt that is reacted by the nonuniform bearing stresses across the thickness. In this paper, when using the Hart–Smith modified NACA TN 1051 equation, composite joint spring rate K is considered to be linearly elastic throughout the loading range. The stiffness comparison for a single-shear flush head fastener joint is shown in Table 1.

NACA 1051 equation[3]:

$$F = C_{bs} + C_{bb} + C_{bbr} + C_{pbr}$$

Hart–Smith modified NACA 1051 equation[4]:

$$F = \frac{1}{K} = \frac{2(t_1 + t_2)}{3G_b A_b} + \left(\frac{t_1 + t_2}{t_1 t_2 E_{bbr}} + \frac{1}{t_1(\sqrt{E_L E_T})_1} + \frac{1}{t_2(\sqrt{E_L E_T})_2}\right)(1 + 3\beta)$$

Double-Shear Joint

In finite element modeling of double-shear joints, bolts are modeled as two bar elements, each connecting the center of the plate to both outer splice plates, as shown in Fig. 4. Each bolt should be modeled with only half of the total spring rate of the joint. As with

Table 2 Stiffness and flexibility comparison for double-shear protruding-head bolt joint

Samples		NACA equation	Lee modified NACA equation	Test data[a]
Isotropic material $t_1 = 0.8$ in. (side member) $t_2 = 0.8$ in. (main member) $D = \frac{9}{16}$ in. Ti. bolt $E_1 = 10.5$E6 psi; Al 2024 $E_2 = 10.5$E6 psi; Al 2024	Flexibility F	1.75E−06	6.03E−06	5.50E−07
	Spring rate K	5.73E+05	1.66E+05	1.82E+06
Isotropic material $t_1 = 0.4$ in. (side member) $t_2 = 0.4$ in. (main member) $D = \frac{3}{8}$ in.Ti.bolt $E_1 = 10.5$E6 psi; Al 2024 $E_2 = 10.5$E6 psi; Al 2024	Flexibility F	2.48E−06	9.14E−07	9.90E−07
	Spring rate K	4.04E+05	1.09E+06	1.01E+06
Composite material $t_1 = 0.25$ in. (side member) $t_2 = 0.5$ in. (main member) $D = \frac{1}{2}$ in. Ti. bolt $E_{1L} = 12.12$E6 psi $E_{1T} = 5.147$E6 psi $E_{2L} = 12.12$E6 psi $E_{2T} = 5.147$E6 psi	Flexibility F	1.92E−06	1.09E−06	1.10E−06
	Spring rate K	5.21E+05	9.14E+05	9.10E+05[a]
Composite material $t_1 = 0.335$ in. (side member) $t_2 = 0.67$ in. (main member) $D = \frac{3}{4}$ in. Ti. bolt $E_{1L} = 12.12$E6 psi $E_{1T} = 5.147$E6 psi $E_{2L} = 12.12$E6 psi $E_{2T} = 5.147$E6 psi	Flexibility F	1.36E−06	7.95E−07	8.16E−07
	Spring rate K	7.38E+05	1.26E+06	1.23E+06[a]
Composite material $t_1 = 0.17$ in. (side member) $t_2 = 0.34$ in. (main member) $D = \frac{1}{4}$ in. Ti. bolt $E_{1L} = 12.12$E6 psi $E_{1T} = 5.147$E6 psi $E_{2L} = 12.12$E6 psi $E_{2T} = 5.147$E6 psi	Flexibility F	3.64E−06	1.80E−06	1.98E−06
	Spring rate K	2.75E+05	5.55E+05	5.05E+05[a]

[a]Test data from Refs. 5 and 6.

single-shear joints, the most widely used flexibility equation for double-shear joints is still from NACA TN 1051 and 1458 (Refs. 3 and 4).

NACA 1051 equation[3]:

$$F = C_{\text{bs}} + C_{\text{bb}} + C_{\text{bbr}} + C_{\text{pbr}}$$

$$F = \frac{2t_1 + t_2}{3G_b A_b} + \frac{8t_1^3 + 16t_1^2 t_2 + 8t_1 t_2^2 + t_2^3}{192E_b I_b} + \frac{2t_1 + t_2}{t_1 t_2 E_{\text{bbr}}} + \frac{1}{t_1(\sqrt{E_L E_T})_1} + \frac{2}{t_2(\sqrt{E_L E_T})_2}$$

Lee modified NACA 1051 equation[6,7]:

$$F = \frac{t_1 - t_2}{5G_b A_b} + \frac{L_{\text{eff}}^3}{12E_b I_b} + \frac{3t_1 + t_2}{3t_1 t_2 E_{\text{bbr}}} + \frac{1.1}{t_1(\sqrt{E_L E_T})_1} + \frac{1.1}{t_2(\sqrt{E_L E_T})_2}$$

where

$$L_{\text{eff}} = t_1/3 + t_2/5$$

To predict the test results accurately, the bolt shear deformation term was reduced by 50%, and the bolt bending deformation term was modified because it was too high, compared to the shear deformation and bearing deformation. In addition, the bolt bearing deformation term was reduced 66% because its deformation was too large, compared to the side member bearing deformation. The bearing deformation term of the main splice was reduced 70%, and the side member bearing deformation term was increased 20% to satisfy the observed physical behavior of the joint deformation. As a result, the Lee modified NACA 1051 equation was developed to accommodate these changes. Tables 2 and 3 summarize the stiffness and flexibility comparisons for double-shear protruding and flush head bolt joints.

Two sets of testing data[5,6] were compared to the predictions from the semi-empirical flexibility equation, and its reciprocal joint spring rates were compared as well. The Lee modified equation matches the experimental data fairly well, whether the jointed materials are metallic or composite. For specimens with bolt diameters larger than $\frac{3}{8}$ in. and smaller than $\frac{1}{4}$ in., the predicting errors from the Lee modified equation are less than 5 and 10%, respectively.

In the case of double-shear joints with flush-head fasteners, predictions from the Lee modified equation matched the tested results relatively well for the metallic bolted joint. No composite material testing data were available for flush-head bolted double-shear joints at this time, although additional testing is desired for inclusion in this comparison study.

The predicted results from the Lee modified equation matched the testing data very well, even for the flush-head fastener specimens with diameters of $\frac{3}{8}$ in., although one joint sample had a 30% difference in spring rate. Unlike single-shear bolted joints, the double-shear joint does not rotate. The preceding comparison shows that the Lee modified equation holds true for the flush-head or protruding head fastener in double-shear bolted joints.

Finite Element Analysis and Failure Prediction

The finite element linear and nonlinear analyses were performed by using NASTRAN software for both compression and tension joint specimens. PATRAN was used in this study as a preprocessor and postprocessor to display the stress–strain contour plots, deflections, and reaction free-body load for all of the components. Finally, the finite element analysis output was transferred to spreadsheets for margins-of-safety calculations. Critical sections of the specimens were discussed in detail, as shown in Ref. 6.

Table 3 Stiffness and flexibility comparison for double-shear flush-head bolt joint

Samples		NACA equation	J. Lee's modified NACA equation	Test data[6]
Isotropic material $t_1 = 0.4$ in. (1.0 cm) (side member) $t_2 = 0.8$ in. (2.0 cm) (main member) $D = \frac{3}{8}$ in. (0.95 cm) Ti. bolt CSK $E_1 = 10.5$E6 psi (72.4 GPa); A1 2024 $E_2 = 10.5$E6 psi (72.4 GPa); A1 2024	Flexibility F	3.28$E-$06	9.57$E-$07	5.50$E-$07
	Spring rate K	3.05$E+$05	1.05$E+$06	1.08$E+$06
Isotropic material $t_1 = 0.4$ in. (1.0 cm) (side member) $t_2 = 0.4$ in. (1.0 cm) (main member) $D = \frac{3}{8}$ in. (0.95 cm) Ti. bolt CSK $E_1 = 10.5$E6 psi (72.4 GPa); A1 2024 $E_2 = 10.5$E6 psi (72.4 GPa); A1 2024	Flexibility F	2.48$E-$06	9.14$E-$07	9.02$E-$07
	Spring rate K	4.04$E+$05	1.09$E+$06	1.11$E+$06
Isotropic material $t_1 = 0.25$ in. (0.64 cm) (side member) $t_2 = 0.4$ in. (1.0 cm) (main member) $D = \frac{3}{18}$ in. (0.42 cm) Ti. bolt CSK $E_1 = 10.5$E6 psi (72.4 GPa); A1 2024 $E_2 = 10.5$E6 psi (72.4 GPa); A1 2024	Flexibility F	2.16$E-$06	1.03$E-$06	1.30$E-$06
	Spring rate K	4.62$E+$05	9.71$E+$05	7.63$E+$05
Isotropic material $t_1 = 0.25$ in. (0.64 cm) (side member) $t_2 = 0.8$ in. (2.0 cm) (main member) $D = \frac{3}{8}$ in. (0.95 cm) Ti. bolt CSK $E_1 = 10.5$E6 psi (72.4 GPa); A1 2024 $E_2 = 10.5$E6 psi (72.4 GPa); A1 2024	Flexibility F	2.57$E-$06	1.04$E-$06	1.10$E-$06
	Spring rate K	3.89$E+$05	9.58$E+$05	9.09$E+$05

Table 4 Bolt torque in composite joint

Fastener size, in. (cm)	DPS 2.70-2 steel bolt, in.-lb (cm-N)	Recommended bolt torque in.-lb (cm-N)	Equivalent joint preload lb (N)
$\frac{3}{8}$ (0.95)	260–320 (2938–3616)	300 (3390)	8,000 (60% bolt Ftu) (35600)
$\frac{1}{2}$ (1.27)	800–1140 (9040–12882)	750 (8475)	15,000 (62% bolt Ftu) (66750)
$\frac{5}{8}$ (1.59)	1845–2120 (20849–23956)	1500 (16950)	24,000 (62% bolt Ftu) (106800)
$\frac{3}{4}$ (1.9)	3840–4080 (43392–46104)	2200 (24860)	29,333 (52% bolt Ftu) (130532)

High-Load Double-Shear Tension Specimen

The double-shear tension specimen model consisted of the skin, stringers, and IML and OML splice plates. The skin and the splice plates were modeled with plates at the midplane and joined by bar elements representing the bolts. This model has two different boundary conditions, the pin at the loaded end and fixed at the spliced end.

Composite Skin Panel

The overall strain fringe plot for the composite skin and stringers was done. Two key areas were identified: the neck transition region and the most highly loaded bolt. Moreover, the maximum strain in the neck transition region was 5870 μ-in./in. (μ-cm/cm). Because the average failure strain of coupons is 10,732 μ-in./in. (μ-cm/cm), this results in a positive margin of safety of 0.83. The bearing load at the most highly loaded bolt was 64 ksi (441.6 MPa). The allowable is 65.8 ksi (454 MPa), which results in a margin of safety of 0.03. Hence, this is the critical failure mode predicted for the tension specimen.

Aluminum Splice Plates

The overall stress fringe plot for the IML splice plate was completed. Because of inherent eccentricity in the test specimen, bending at the center of the main splice plate is the cause of peak stress over the entire surface. A peak stress of 45 ksi (310.5 MPa) occurs at the extreme surface against the composite, and a stress of 51 ksi (351.9 MPa) occurs on the outer surface. The ultimate tensile strength of the aluminum splice plate is 83 ksi (572.7 MPa). Thus, the margins are 0.84 and 0.63 respectively at these surfaces. The aluminum OML splice plate is connected by the same bolts that connect the IML splice plate, thereby sandwiching the composite skin with four rows of bolts.

Steel Bolt Connection

Friction effects were not considered in the high-load tension FEM. Therefore, all of the applied loads are transferred through bolt connections. The bolt free-body loads were mapped at the bolt connection joints in this finite element model. This preliminary FEM was constructed assuming there was no clamp-up torque (preload) in the joint. However, the bolt clamp-up force is vitally important for the bolt connection joint. As the result of a recent study, the torque values presented in Table 4 are recommended. All of the bolt tension allowables are summarized in Refs. 6 and 7.

High-Load Single-Shear Compression Specimen

A finite element analysis for the single-shear compression specimen was done. The detail shell model consists of the skin, stringers, IML splice plate, and OML flex tee. The skin, the IML splice plate, and OML flex tee are modeled with plates at the midplane and joined together by bar elements representing the bolts. The stress level of a 0.4-in. (1 cm) forced displacement at one end and is equivalent to 1444 kip (6425800 N) axial compression loading in the specimen. The boundary conditions for the linear and nonlinear analysis are the same and have a fixed-fixed condition to stimulate the test step. However, the buckling analysis model has different boundary conditions (pin-pin) to represent the actual wing skin and rib structures.

Composite Skin Panel

The overall strain fringe plot for the composite skin and stringers was done. Two key areas were identified: the minimum gauge transition region and the region surrounding the most highly loaded bolt. The margin of safety for a high-load single-shear compression specimen is 0.06. Hence, this is the critical failure mode predicted for the compression specimen.

Aluminum Splice Plate

The overall stress fringe plot for the main splice was done. Because of inherent eccentricity in the test specimen, severe bending at the center of the main splice plate caused high peak stress over the entire surface. The splice plate shows a peak stress of 67 ksi (462.3 MPa) at the extreme surface, including the bending as well as axial compression stresses. The ultimate compression strength of the aluminum splice plate is 83 ksi (572.7 MPa), and hence the margin of safety is 0.24.

Aluminum Flex Tee Plate

The overall stress fringe plot for the flex tee plate was done. The flex tee is connected to the composite skin by the last two lines of bolts on each side. Hence, it shares some of the bolt loads with the main splice plate. It has a constant thickness of 0.25 in. and is designed as a flexible member that will allow the pressurized fuselage to expand. In addition, it is designed to share the bolt loading and to minimize the eccentricity at the center. From the results of the finite element analysis, the flex tee will yield until a 2% elongation takes place. The ultimate compression strength of the aluminum flex tee is 83 ksi and has an 8% ultimate elongation allowable before the final rupture takes place.

Steel Bolt Connection

Friction effects were not considered in the high-load compression specimen finite element model. The free-body loads at the bolt connection joint, and the recommended torque values, should follow those listed in Table 4. All of the detailed numerical calculations and the related figures of the finite element analysis are presented in Ref. 6.

Test Verification

The test setup for the high-load tension specimen was not available at this time. However, actual testing was conducted to verify this high-load compression bolted panel. The panel will be statically loaded in compression to failure between two flat and parallel plates in a 1.5 million-lb loading frame.

The high-load compression specimen was tested statically to failure. It failed at a load of 1206 kips, which is equivalent to a 50.1 kips/in. running load. Figure 5 shows a plot of the applied load vs the cross-head displacement. This curve shows an initial nonlinearity, which is attributed to the test frame and settling of the specimen, followed by linear behavior until the load reached 1050 kips, then slightly nonlinear behavior developed just prior to failure. Figure 6 shows the strains from representative gauges on the OML and IML surfaces of the composite skin, from gauges on the flex tee, and gauge sites on the splice plate. The gauges on the flex tee and splice plate reveal the initiation of a nonlinear response at 700 kips.

The past test examination revealed fiber and interlaminar failures in the skin and stringers of the upper composite panel, as shown in Fig. 7. The fiber failure in the skin ran all of the way across the composite beneath the outer stringers and through the center stringer, as shown schematically in Fig. 8. The examination also revealed that the two outer stringers of the upper panel were delaminated from the skin.

The failure was at 1206 kips, which is the design load of 50 kips/in. However, it was 17% below the analytically predicted strength of the composite bolted joint. The dramatic changes in the strains just prior to failure suggest the development of significant bending moments created from the initiation of instability. If the specimen buckled into a full wave mode, this would be consistent with the essentially clamped end conditions and the changes in strains observed in composite and splice plates. Even though these explanations match the data and observations, additional analysis is needed before definitive conclusions are drawn.

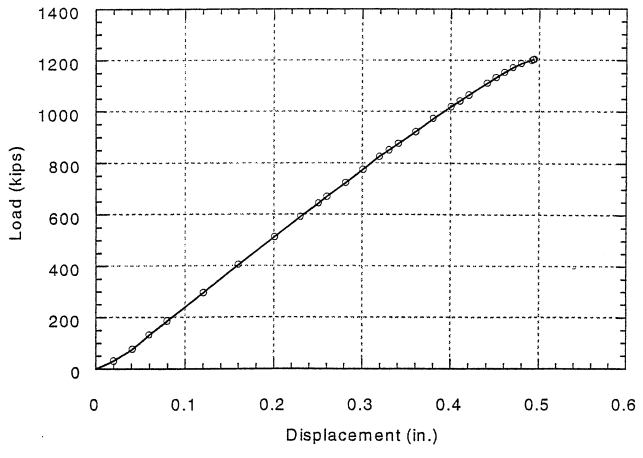

Fig. 5 Load-displacement response of the high-load compression specimen.

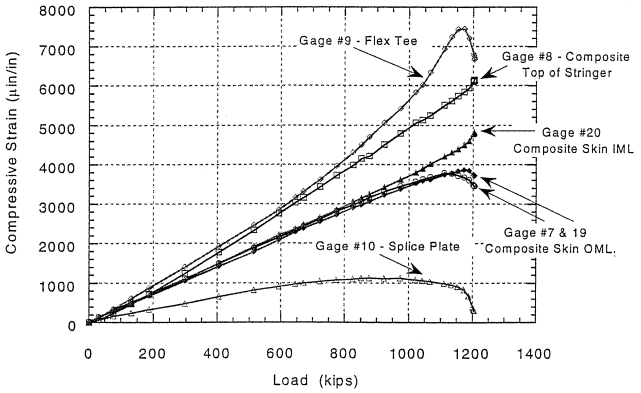

Fig. 6 Measured compressive strains as a function of load for selected gauges.

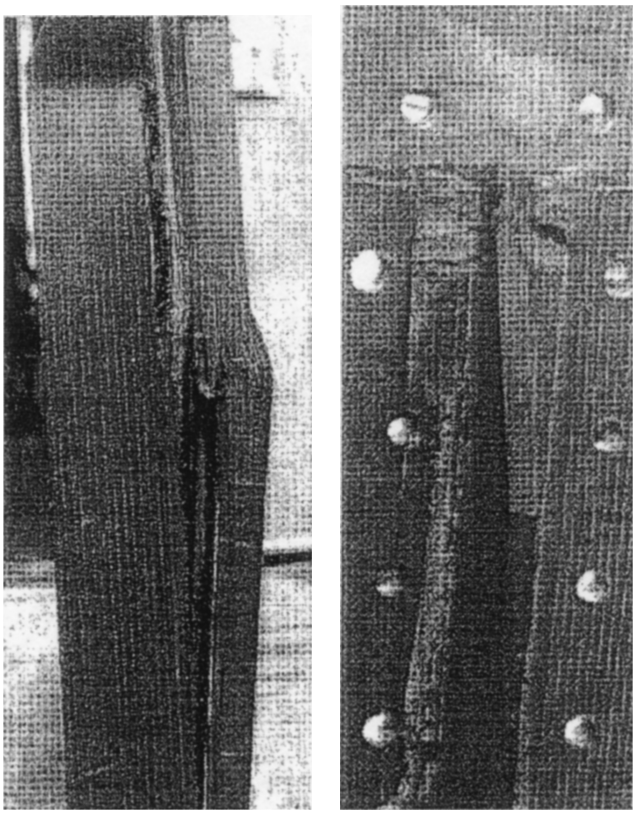

a) **b)**

Fig. 7 Photographs of the upper S/RFI composite panel showing the failure damage: a) side view showing failure in the skin and the debonding between the stringer flange and the skin b) close-up of the delamination of one of the outer stringers.

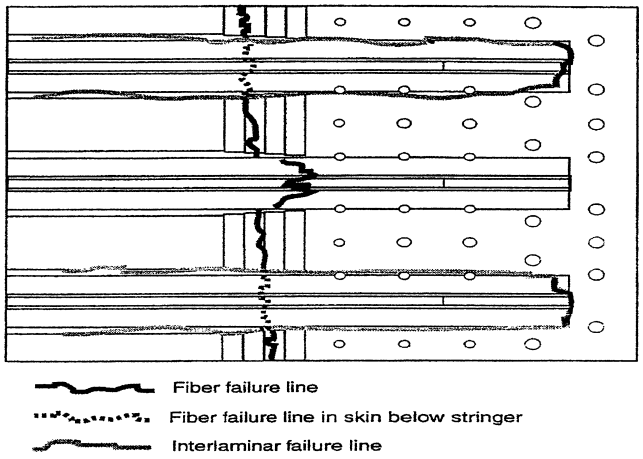

Fig. 8 Schematic of the fiber and interlaminar failure locations in the specimen.

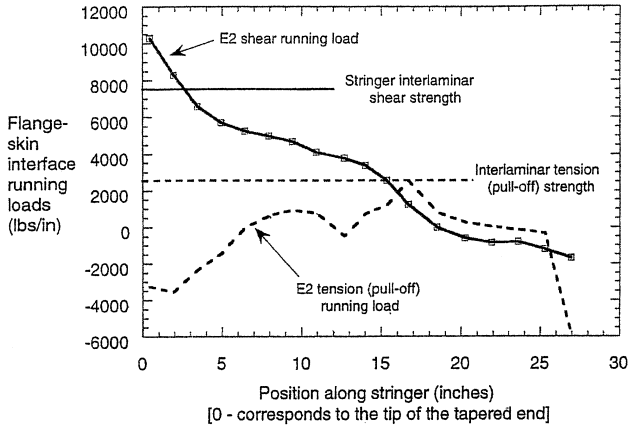

Fig. 9 Interlaminar tension and shear running loads obtained from the finite element analysis of the high-load compression specimen and compared to the tension and shear interlaminar strength findings from the actual test.

After the test the tension and shear running loads at the interface between the stringer flange and the skin predicted by the finite element analysis were examined. These are plotted in Fig. 9, along with the applicable tension and shear interlaminar strengths. The predicted tension running loads are below the interlaminar tensile strength, along the entire length of the stringer, but the predicted shear running loads exceed the interlaminar shear strength for the first 2–3 in. This suggests that the failure of the high-load compression specimen might be initiated by an interlaminar shear failure at the interface between the stringer flange and the skin. Such a failure would severely reduce the bending resistance of the panel and promote instability and significant bending moments in the panel, which is consistent with the strain and gauge readings just presented.

Conclusions

The development of effective methods for the design, analysis, and evaluation of multirow highly loaded bolt joints is an important task for the successful implementation of composite structures for aircrafts. This study describes the method of analysis for highly loaded bolted joints in composite wing structures. The designed specimens were made of stitched/resin film-infused carbon fiber composite material, and their load intensities were on the order of 50 to 60 kips/in. (87598.5 to 105118.2 N/cm), within the specimen width for 0.94-in. (2.39 cm)-thick pad-up skin.

From the finite element analysis the critical margin (0.06) corresponds to a bearing-bypass failure in the composite at the first row of bolts. Thus, failure of the high-load compression specimen was predicted to occur at the first row of bolts at a load above the 1444 kips (6425800 N). However, the high-load compression specimen failed at a load of 1206 kips (4565700 N) and carried a peak running load of 50 kips/in. (87598.5 N/cm) The compression specimen failed at 50 kip/in. (87598.5 N/cm) because of deflections. The deflection induces secondary bending moments, which resulted in a high interlaminar shear flow between the skin and stringers. The stitch helped the composite structure, but it was not enough. The strength of the bolted joint was much greater than the interlaminar strength of the skin-stringer interface.

In the design and analysis of multirow highly loaded bolt joints in composite wing structures, uniform bolt loading is crucial to the joint design and vigorous flexibility calculations, as shown in this study. The preliminary, modified NACA 1051 semi-empirical equation indicated a good improvement in predictions for specimens with bolt diameters larger than $\frac{3}{8}$ in. (0.95 cm), irrespective of whether or not the jointed materials are metallic or composites. However, because of the highly nonlinear stress distribution inside the bolt joints, and the anisotropic behavior of the composite materials, further investigation of these bolt joint problems, via both experimental and theoretical approaches, is imperative.

Acknowledgments

The authors wish to express their sincere appreciation for the testing arrangements and results provided by the McDonnell Douglas Aerospace Company. Appreciation is also extended to those people who have contributed to making this study possible. The last author is supported by the special topic research grant from the I-Shou University (Grant ISU 92-02-19).

References

[1]Swift, T., "Repair to Damage Tolerant Aircraft," International Symposium on the Structural Integrity of Aging Airplanes, March 1990.

[2]"Design of the B-1 Composite Horizontal Stabilizer Root Joint," NASA TM X-3377, April 1976.

[3]NACA TN 1051, Dec. 1945.

[4]NACA TN 1458, Oct. 1947.

[5]Hart-Smith, L. J., and Bunin, Bruce, L., "Critical Joints in Large Composite Aircraft Structure," Douglas Paper 7266, Jan. 1983.

[6]Lee, J. J., "Design and Analysis of Multi-Row Highly Loaded Bolt Joints in Composite Wing Structures," M.S. Thesis, Dept. of Mechanical Engineering, California State Univ., Long Beach, CA, May 2000.

[7]"Threaded Fastener Flexibility Test–TWR L350," Development Release Order, DRO-706772, July 1999.